Hindawi Publishing Corporation
Journal of Sensors
Volume 2016, Article ID 2183569, 13 pages
http://dx.doi.org/10.1155/2016/2183569

Review Article

The Brief Introduction of Different Laser Diagnostics Methods Used in Aeroengine Combustion Research

Fei Xing,[1] Yue Huang,[1] Mengmeng Zhao,[2] and Jian Zhao[3]

[1] *Department of Aeronautics, School of Aerospace Engineering, Xiamen University, Xiamen, Fujian 361005, China*
[2] *Faculty of Engineering and Surveying, University of Southern Queensland, Toowoomba, QLD 4350, Australia*
[3] *Science and Technology on Metrology and Calibration Laboratory, Changcheng Institute of Metrology & Measurement, Beijing 100095, China*

Correspondence should be addressed to Fei Xing; f.xing@xmu.edu.cn

Received 20 October 2015; Revised 13 December 2015; Accepted 11 January 2016

Academic Editor: Zhida Xu

Combustion test diagnosis has always been one of the most important technologies for the development of aerospace engineering. The traditional methods of measurement have been unable to meet the requirements of accurate capture of the flow field in the development process of the aeroengine combustor. Therefore, the development of high-precision measurement and diagnostic techniques to meet the needs of the aeroengine combustor design is imperative. Laser diagnostics techniques developed quickly in the past several years. They are used to measure the parameters of the combustion flow field such as velocity, temperature, and components concentration with high space and time resolution and brought no disturbance. Planar laser-induced fluorescence, coherent anti-Stokes Raman scattering, tunable diode laser absorption spectroscopy, and Raman scattering were introduced systemically in this paper. After analysis of their own advantages and disadvantages, the authors considered validated Raman scattering system and Tunable Diode Laser Absorption Tomography are more suitable for research activities on aeroengine combustion systems.

1. Introduction

The development of gas turbine technology is crucial for national security, energy security, and environment protection. For both engines for military airplane (pursuing for high thrust-weight ratio) and ground civilian gas turbine (pursuing for high thermal efficiency), the goal is to increase the pressure ratio for high thermal efficiency and the combustor exhaust temperature for high specific thrust [1–3], which requires precise measurement and diagnostic technology.

Traditional measurement methods, such as thermal couples for temperature measurement and gas chromatographer for species concentration in the gas measurement, generally need probes to obtain the sample gas, which could disturb the flow field, and may cause shockwaves in supersonic flow field or catalytically react with sample species [4, 5]. At the same time, the turbulent flow field in the gas turbine combustor is so complicated that it leads to another shortcoming of traditional diagnostic tools; it is hard to setup and capture the detailed flow field information inside the combustor. The deficiency and inaccuracy of the traditional measurement technology have become the obstacle for the development of advanced aeroengines.

The laser diagnostic tools are superior over traditional contacting tools, because they bring no disturbance to the flow field. The laser measurement technology will be also able to extend the traditional point measurement to the line or plane measurement. Because of these merits, the laser measurement technology would help to measure and obtain the information of the detailed transient combustion flow field inside the combustor and has been recognized and applied in the design and development process of the gas turbines [6]. This paper will introduce four different popular laser diagnostic methods, which have little influence on the flow field but with very high accuracy.

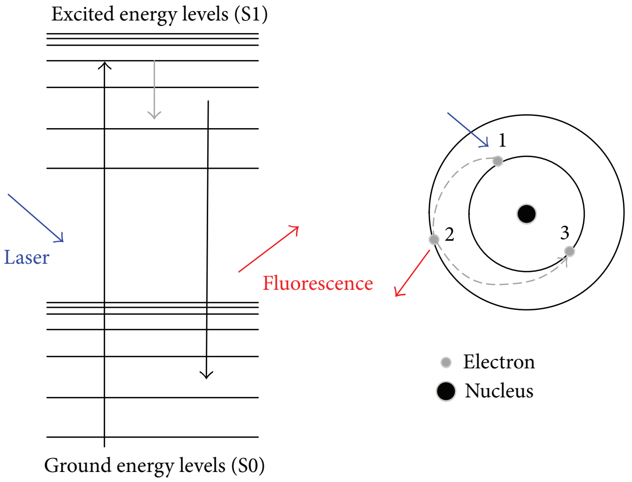

Figure 1: Basic principles of PLIF.

2. Planar Laser-Induced Fluorescence (PLIF)

Planar laser-induced fluorescence (PLIF) is an optical diagnostic technique widely used for flow visualization and quantitative measurements. It has been shown to be used for velocity, concentration, temperature, and pressure measurements in [7]. In PLIF measurement system, the flow field is illuminated by a laser light sheet whose wavelength tuned to excite a particular transition; please see Figure 1. A fraction of ground state molecules of the flow absorb the incident light and are excited to a higher electronic energy state. The excited species exist only in the order of a few nanoseconds to microseconds; afterwards the excited species deexcite and emit light at a wavelength larger than the excitation wavelength, which can be captured by a digital camera.

A typical PLIF system consists of a source of light (usually a laser), an arrangement of lenses to form a sheet, fluorescent medium, collection optics, and a detector. The light from the laser (usually a beam) passes through a set of lenses and/or mirrors to form a sheet, which is used to illuminate the medium. This medium either is made up of fluorescent material or can be seeded with fluorescent substance. The signals are usually captured by a CCD or CMOS camera and can be related to various properties of the medium.

One important application of PLIF is the combustion-LIF system. The system employs a laser light source with light sheet optics to illuminate a thin plane of the combustion process. The laser wavelength is tuned to correspond to an energy transition within the molecular species of interest, resulting in absorption of the light, thus leading to excitation of some of the molecules to a higher electronic energy state.

Due to collisions between the molecules in the gas, a redistribution of energy occurs immediately after the excitation, causing a population of closely adjacent energy states, subsequently returning to a lower energy state with a part of the excess energy released as photons, which is commonly known as fluorescence.

As a result of the energy redistribution, the fluorescence is to a large extent shifted towards longer wavelengths, relative to that of the excitation. Detection of the fluorescence is generally done at these red-shifted wavelengths so as to minimize interference from scattered laser light [7]. A spectral filter is placed in front of the camera lens, allowing only the fluorescence to reach the intensified camera.

In 1990, McMillin et al. used PLIF technology to measure the structure of shock by heat flow imaging of NO in shock tube [8]. In 1999, Frank et al. get the imagines of OH in the aeroengine combustor chamber under different pressure (maximum test pressure is 2026.5 kPa) by using PLIF technology [9]. In 2002, Hanson used PLIF technology to study the supersonic combustion [10]. In 2005, Seyfried et al. measured the residual fuel concentration and temperature distribution in afterburner of RM12 engine by PLIF and LIP technology [11].

Compared with other techniques, PLIF has its own advantage. For example, PLIF can be combined with Particle Image Velocimetry (PIV) to measure the species concentration and velocity simultaneously [12]. A PLIF and PIV optical system can be seen in Figure 2. But there are also some limitations for this kind of technology; for example,

(i) the measured flow field must contain molecular species with an optical resonance wavelength that can be accessed by laser;

(ii) temperature measurements typically require two laser sources;

(iii) velocity measurements are usually practical only for high Mach number flows (near sonic or supersonic);

(iv) signal-to-noise ratio is often limited by detector shot-noise;

(v) fluorescence interferences are from other species, especially from hydrocarbons in high pressure reacting flows.

3. Coherent Anti-Stokes Raman Scattering (CARS)

Coherent anti-Stokes Raman scattering, also called coherent anti-Stokes Raman spectroscopy, is a form of spectroscopy used primarily in chemistry, physics, and related fields [13]. It is a nonlinear four-wave mixing process that is used to enhance the weak (spontaneous) Raman signal.

As shown in Figure 3, in the CARS process, a pump laser beam (at frequency ω_{pump}) and a Stokes laser beam (at ω_{Stokes}) interact, producing an anti-Stokes signal at frequency $\omega_{\text{CARS}} = 2\omega_{\text{pump}} - \omega_{\text{Stokes}}$. The Stokes beam ($\omega_{\text{Stokes}}$) is typically provided by a 1064 nm line from an Nd:Vanadate laser. This Nd:Vanadate laser also acts as the pump source for an optical parametric oscillator (OPO), while the output from the OPO (680–1010 nm) acts as the pump beam (ω_{pump}). When the frequency difference (beat frequency) between the pump and the Stokes beams matches the frequency of a (Raman active) vibrational mode, such as the CH_2 symmetric stretching

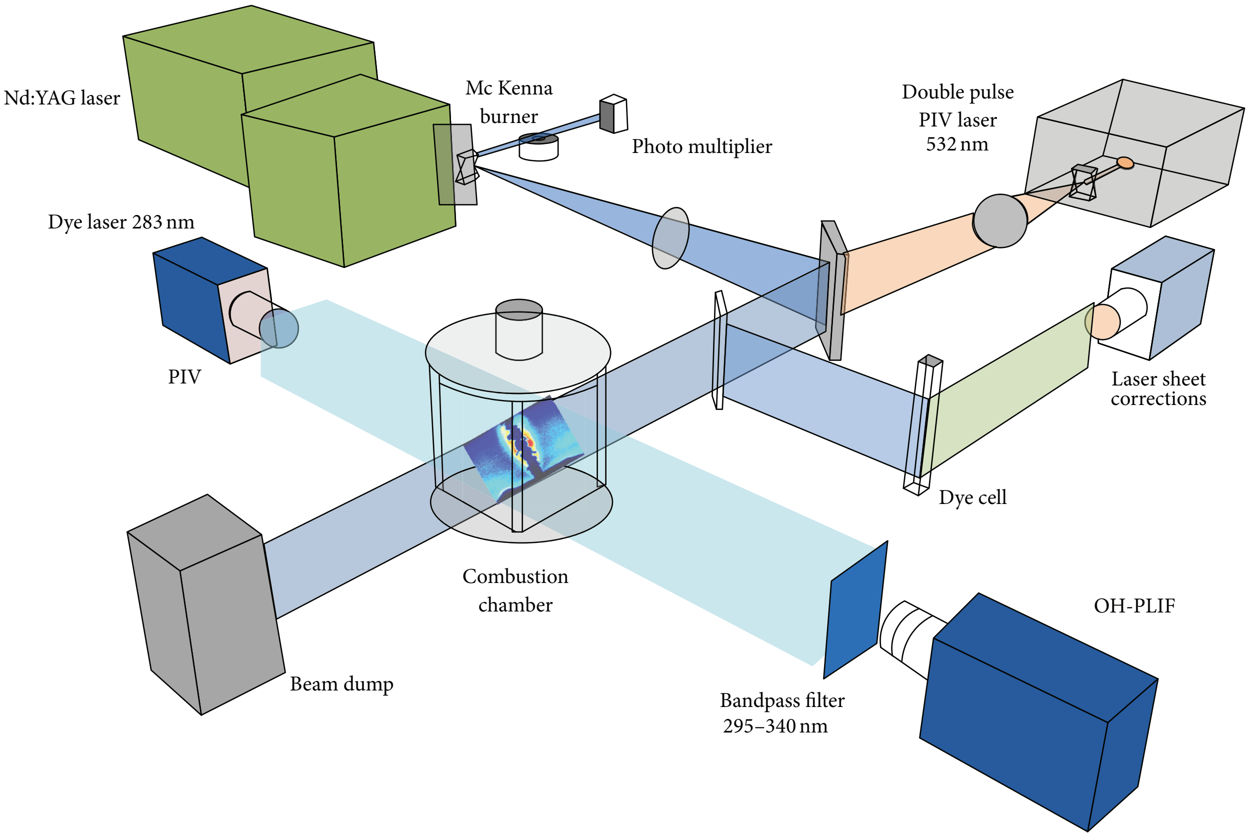

Figure 2: Schematics of the optical system used for simultaneous OH-PLIF and PIV measurements [12].

mode at 2800 cm^{-1}, the molecular oscillators are coherently driven [14]. This results in an enhanced anti-Stokes (shorter-wavelength) Raman signal that is the basis for the increased vibrational contrast of CARS.

Using the CARS method with a broad pump probe and a narrow Stokes band, it allows us to excite multiple vibrational coherences at once. This method has been utilized to investigate vibrational responses around 3000 cm^{-1}. Using a high resolution phase shaper to scan a p-phase step through the broadband pump/probe spectrum, it is able to obtain nonresonant background-free CARS spectra with a resolution of 1 cm^{-1}. The nonresonant background is removed by using the inverse phase-profile signal from the original scan, exploiting the time-reversal asymmetry of the resonant signal.

CARS is now often compared to Raman scattering as both techniques probe the same Raman active modes. The differences between signals from Raman and CARS stem largely from the fact that Raman relies on a spontaneous transition while CARS relies on a coherently driven transition [15]. Given the fact that CARS is a higher order nonlinear process, the CARS signal from a single molecule is larger than the Raman signal from a single molecule for a sufficiently high driving intensity. However, at very low concentrations, the advantages of the coherent addition for the CARS signal are reduced and the presence of the incoherent background becomes an increasing problem.

NASA Langley Research Center (LRC) and United Technology Research Center (UTRC) are main organizations to promote the development of CARS technology and its applications [16–19].

During 1980–1995, the applications of CARS on the combustion flow field in aeroengine combustor, supersonic combustion flow field in scramjet, and the combustion flow field with solid propellant were studied. Except obtaining the preliminary results of the measurement, the research also included the feasibility study of CARS in the actual engine combustion diagnosis, measurement scheme design, and noise processing. The results of the study also showed that there were many factors that could affect the measurement results, such as laser mode and pulse time characteristic.

After 1999, some new research topics were developed; for example, a multiphoton microscopy based on coherent anti-Stokes Raman scattering is accomplished with near-infrared ultrashort laser pulses for 3-vibrational imaging, which was with high sensitivity, high spatial resolution, noninvasiveness, and three-dimensional sectioning capability [20, 21] (Figure 4).

In conclusion, CARS has several obvious advantages:

(i) Due to the anti-Stokes shift, the CARS signal is of shorter wavelength than one-photon fluorescence.

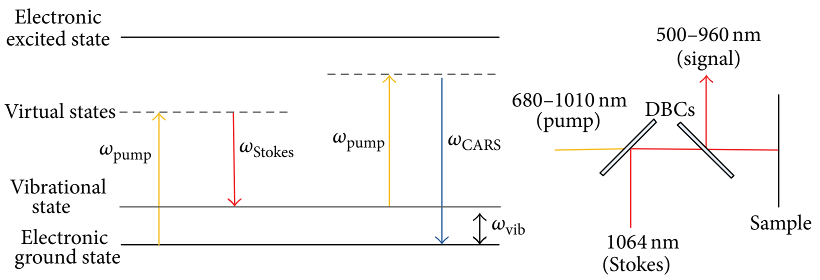

Figure 3: Coherent anti-Stokes scattering (CARS) energy diagram and schematic of the experimental setup.

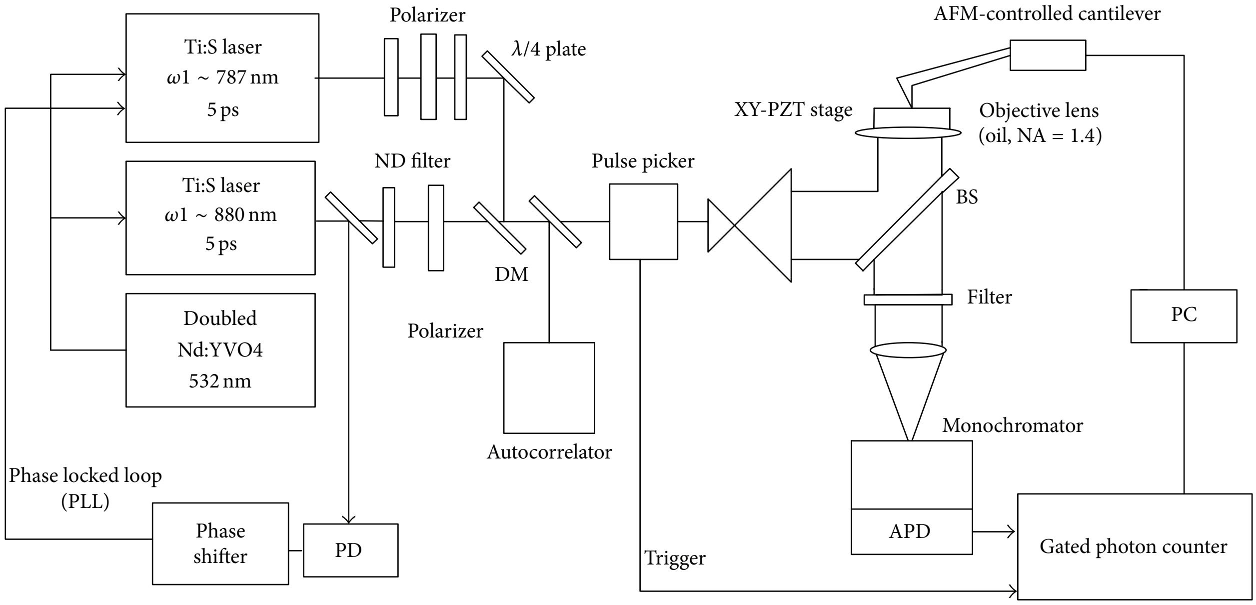

Figure 4: Schematic of the tip-enhanced CARS microscope [21].

This allows detection in the presence of a strong fluorescent background.

(ii) Coherent addition of CARS fields generates a large signal. Nonlinear dependence on excitation intensities produces inherent 3D resolution.

(iii) Low absorption of the near-infrared excitation beams would significantly reduce the damage in samples.

4. Tunable Diode Laser Absorption Spectroscopy (TDLAS)

4.1. TDLAS. Tunable diode laser absorption spectroscopy (TDLAS) is a technique used to measure the concentration of certain species such as methane and water vapor. TDLAS is by far the most common laser based absorption technique for quantitative assessments of species in gas phase [22, 23].

As shown in Figure 5, a basic TDLAS setup consists of a tunable diode laser light source, transmitting optics, an optically accessible absorbing medium, receiving optics, and detectors. The emission wavelength of the tunable diode laser is tuned over the characteristic absorption lines of a species in the gas [24]. This causes a reduction of the measured signal intensity, which can be detected by a photodiode, and then can be used to determine the gas concentration and other properties as described later.

TDLAS system has often been used to measure CO and CH_4 on an aircraft platform. The airborne spectrometer known as DACOM (differential absorption carbon monoxide monitor) uses two independent laser channels to access simultaneously the absorption lines from CO and CH_4 in the 4.7 and 7.6 μm regions, respectively. These airborne measurements are extremely useful in characterizing the geographical distribution of both gases, detecting the chemical signature of biomass plumes conveyed by long range transportation, identifying air mass changes and their potential origins, and studying vertical transport.

The advantage of TDLAS over the other techniques for concentration measurement is its ability to achieve very low detection limits. Apart from concentration, it is also possible to determine the temperature, pressure, and velocity.

The main disadvantage of TDLAS is that this kind of technology highly depends on the measurement of a small change of a signal on top of the background. Any noise introduced by the light source or the optical system will deteriorate the detectability and precision of this technique.

There are basically two ways to improve on the situation: one is to reduce the background noise, and the other is

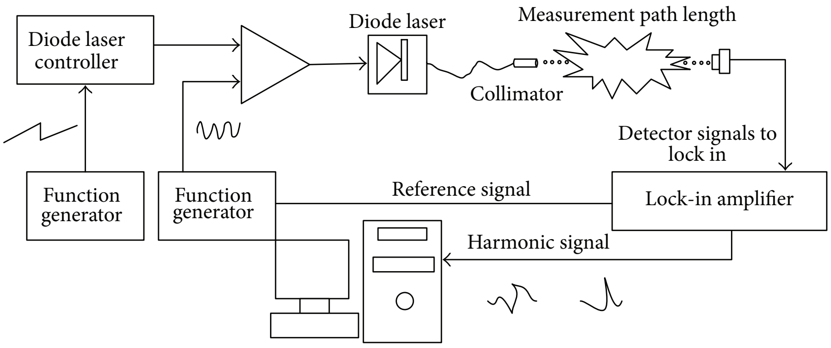

FIGURE 5: A basic setup of TDLAS system.

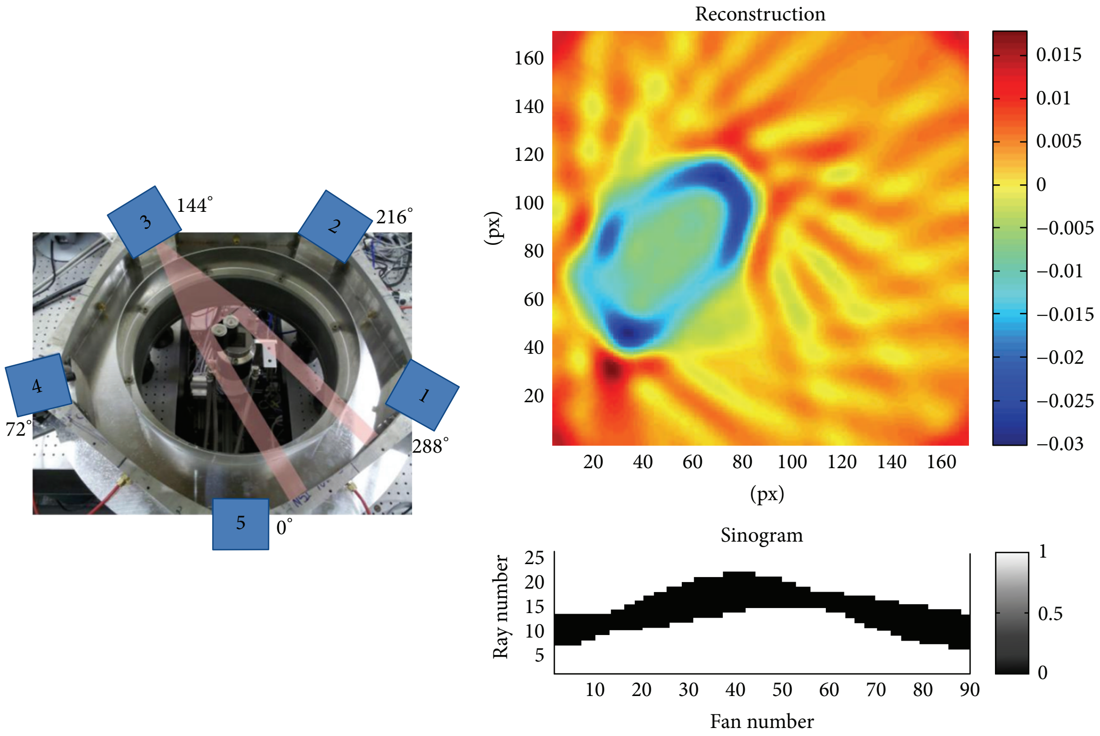

FIGURE 6: TDLAT system mounted to NASA Langley flat flame burner. Opaque object positioned on burner surface [27].

to increase the absorption sensitivity. The former can be achieved by the use of a modulation technique, and the latter one can be obtained by placing the gas inside a cavity in which the light passes through several times, thus increasing the interaction length. If the technique is applied to trace species detection, it is also possible to enhance the signal by performing detection at wavelengths where the transitions have larger line strengths, for example, using fundamental vibrational bands or electronic transitions.

4.2. TDLAT. TDLAS is a path-integrated line-of-sight (LOS) measurement and thus does not produce spatially resolved distributions. Recently, a new relative technology, Tunable Diode Laser Absorption Tomography (TDLAT), combines TDLAS with computed tomography (CT) which have been developed [25–27]. It is a nonintrusive measurement technique for determining two-dimensional spatially resolved distributions of temperature and species concentration in high enthalpy flows. Unlike TDLAS, the TDLAT technique results in a 2D spatially resolved measurement plane. Over 2500 individual TDLAS LOS measurements are collected at numerous locations surrounding the flow of interest and then mathematically reconstructed using MATLAB's ifanbeam tomographic inversion algorithm.

Theory for the TDLAT system is comprised of absorption spectroscopy and computed tomography techniques. First, absorption spectroscopy theory is utilized to analyze and prepare the collected data for tomographic inversion. Second, computed tomography is used to reconstruct the two-dimensional absorbance fields. Lastly, absorption spectroscopy theory is again utilized to obtain the thermodynamic properties of interest at each spatial location [27].

Figure 6 shows the TDLAT system was tested on a NASA Langley flat flame burner. The measurement of an opaque object was performed and the sonogram and the tomographic reconstruction of the opaque object were showed in the figure.

The Beer-Lambert law expresses the relationship between the transmittance of light through a gas mixture and the resulting optical absorption of individual species. The Beer-Lambert law states that the transmittance, T_ν, which is the ratio of the transmitted intensity, I, to the incident intensity, I_0, is proportional to the exponential of the product of path length, L [cm], and κ_ν, the spectral absorption coefficient [cm] of the absorbing species:

$$T_\nu = \frac{I}{I_0} = \exp\left(-\kappa_\nu L\right), \tag{1}$$

where $\kappa_\nu L$ is termed the absorbance. The spectral absorption coefficient is given by

$$\kappa_\nu = S(T) \cdot \phi_\nu \cdot N_T, \tag{2}$$

where $S(T)$ is the transition line strength [cm^{-1}/molecule-cm^{-2}], N_T is the number density of the absorbing species [molecules cm^{-3}], and ϕ_ν is the lineshape function [cm] approximated by a Voigt function. The Voigt function is the spectral lineshape resulting from the convolution of independent Doppler and Lorentzian line broadening mechanisms.

When applied to a supersonic combustor model with hydrogen injection, TDLAT can be utilized to gain understanding of the combustion efficiency. The spatially resolved water vapor concentration resulting from the TDLAT technique can be combined with stereoscopic PIV (which results in 3D velocity vectors) and thus the water vapor flux can be calculated. This measured flux, when compared to the known injected hydrogen flux, can be used as a direct measurement of combustion efficiency in hydrogen-air combustors. This approach is described by the following equation:

$$\eta_c = \frac{\int_{A_{\text{exit}}} n_{\mathrm{H_2O}}(y,z)\, V_x(y,z)\, dA_{\text{exit}}}{\dot{N}_{\text{Hydrogen,injected}}}, \tag{3}$$

where $n_{\mathrm{H_2O}}(y,z)$ is the spatially resolved water number density distribution from the TDLAT measurement, $V_x(y,z)$ is the axial velocity distribution from the SPIV measurement, and $\dot{N}_{\text{Hydrogen,injected}}$ is the total hydrogen flux injected into the combustor.

5. Raman Scattering (RS)

5.1. Principle of Raman Scattering. The molecule elastic scattering of laser photon is Rayleigh scattering. For Rayleigh scattering, there is no energy exchange between the molecule and photon, and the scattering photon has the same frequency as the income laser, but the scattering photons spread in all directions. However, Raman scattering is the result of inelastic collision between molecule and incoming laser photon. There is energy exchange between laser photon and the scattering photon, so the scattering photon has a different frequency to the laser photon.

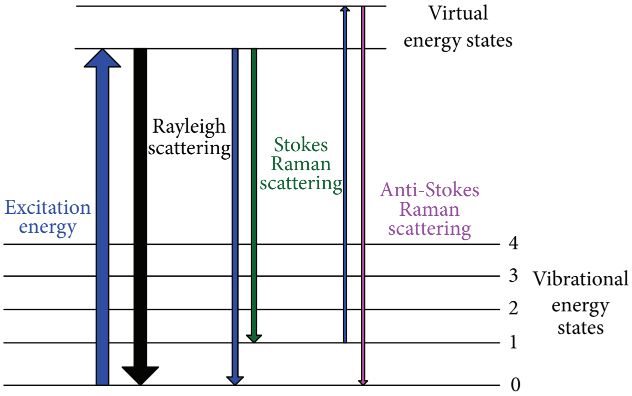

FIGURE 7: Rayleigh and Raman scattering process.

Theoretically, molecule has Raman scattering with any incoming light with enough frequency; a high power single frequency laser is needed for generating enough scattering signal practically. The laser source can be a visible laser or a ultraviolet laser. The Raman scattering with visible laser is called visible Raman scattering, and vice versa, for UV Raman scattering. It is called Stokes scattering if the incoming laser photon loses energy and scatters lower frequency photon, so it is same for the anti-Stokes scattering.

Quantum mechanics has shown that the energy of the gas molecule is not continuous and energy level is discrete. The energy levels of other energy modes are obviously discrete. During the collision of photon and molecule with energy exchange, the vibration and rotation energy level of some molecules change and this molecule energy change is equal to the energy difference between the scattering photon and the incoming photon. Since different molecules have different vibration and rotation energy level, the Raman scattering frequency shifts are different. This frequency shift can be used to identify different species in the fluid. Meanwhile, the Raman scattering signal is proportional to the number density of the species. So the Raman scattering technology can be used to measure different species concentration simultaneously. In the practical laser diagnostics, the vibration frequency shift is often used, because the vibration energy level is large and frequency shift is easily observed.

Figure 7 shows the energy exchange scheme for the above-mentioned Rayleigh and Raman scattering. The size of the arrow represents the strength of the scattering signal. The Raman scattering signals are obviously less than that of Rayleigh scattering; so the Rayleigh signal should be filtered out in the Raman scattering signal collection. The Stokes Raman scattering signal is much stronger than that of anti-Stokes scattering signal. That is why the Stokes Raman scattering is used for laser diagnostics.

The signal intensity of Stokes Raman scattering is

$$I_{\text{Raman}} = C(T) \cdot \sigma \cdot L \cdot N \cdot I. \tag{4}$$

$C(T)$ is the temperature-dependent calibration factor, σ is the Raman scattering cross section, L is the length of the laser

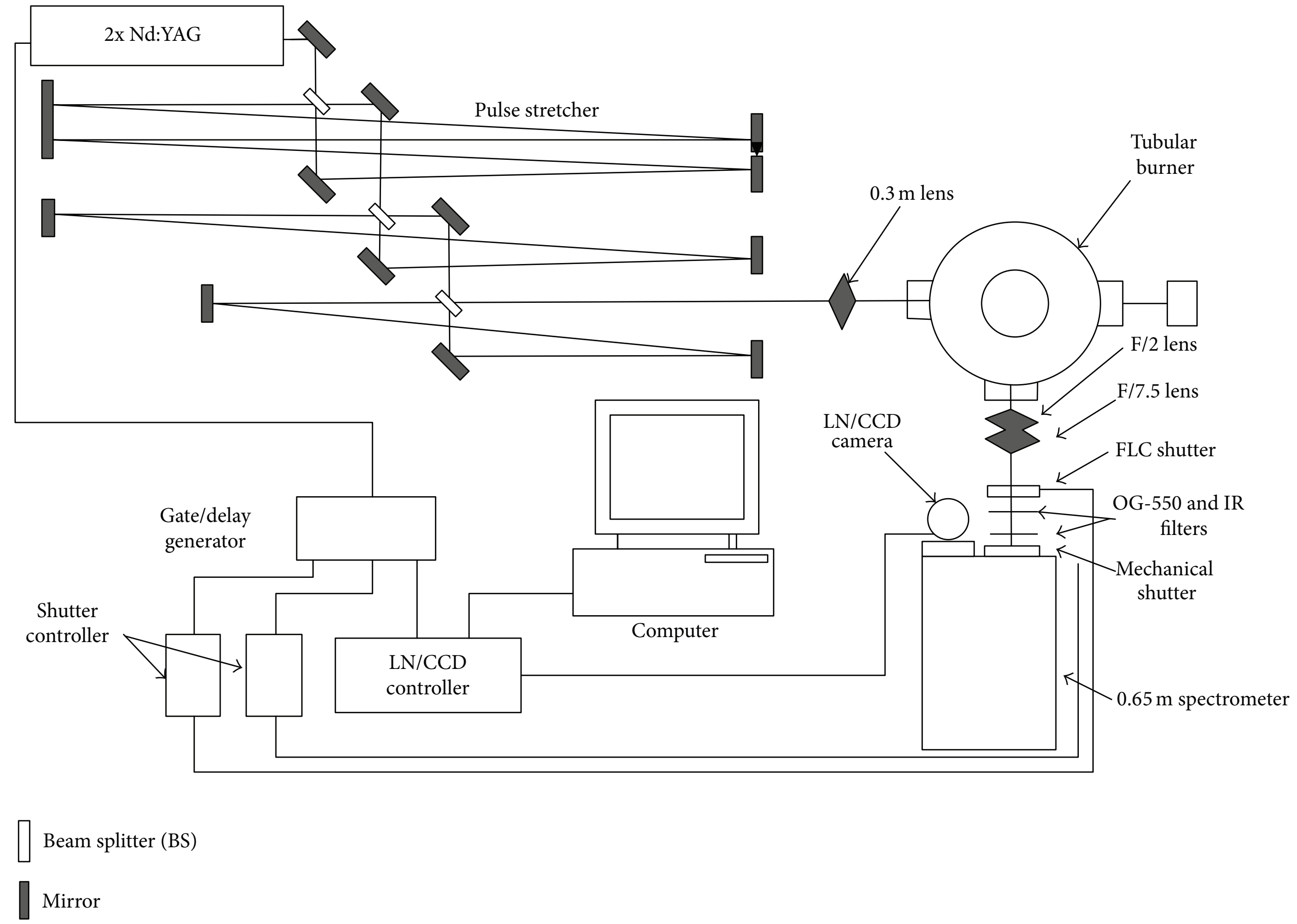

Figure 8: Schematic of the visible Raman system in Vanderbilt University.

beam, N is gas species number density, and I is the laser energy. Also $\sigma \propto \lambda^{-4}$, and the smaller the laser wavelength (the higher the laser frequency), the stronger the scattering signal. That is why the UV Raman scattering is much more attractive than the visible Raman scattering. The signal of UV Raman scattering is strong enough to make it suitable for single shot measurement, broadening its application to resolve the transient behavior of the turbulent reacting flow, while the visible Raman scattering signal is much stronger now than ever before, because of development of the high power laser source, and it may be generally suitable for both transient and steady flow field measurement.

5.2. Validation and Application of Raman Scattering System. At present, there is no commercial Raman scattering system for sale and experienced experimentalists are needed to build and operate this kind of expensive system. The Laser Diagnostic Lab at Vanderbilt University has both the visible and UV Raman scattering systems [28]. A brief description of their visible Raman scattering system in Figure 8 is as follows.

The laser is a frequency-doubled, pulsed Nd:YAG laser (532 nm, 7 ns long @ 10 Hz). The laser beam passes through a zero-order wave-plate mounted at the exit of the laser followed by a thin film plate polarizer at its Brewster angle to enable continuous adjustment of the laser energy. The attenuated beam then goes through a pulse stretcher. By using 3 beam splitters, the laser beam is split into 3 sets of beams trapped in the 3 optical ring cavities with different amount of delay. A laser pulse approximately 150 ns long is produced. The laser light is focused by a 300 mm focal length lens. The scattered Raman light is collected at 90° using an F/2 achromat (3″ diameter) focused by a second achromat (F/7.5) onto the entrance slit of the spectrometer. The focused signal is collimated by a defocusing mirror, and then the signal is dispersed by a liquid-nitrogen-cooling, back-illuminated CCD camera. The CCD camera is gated by a ferroelectric liquid crystal shutter and a mechanical shutter to reduce the background flame emission. The Rayleigh scattered light is blocked by an OG-550 orange glass filter, and the flame illumination in the infrared region is blocked by an infrared filter.

The calibration and validation of the Raman system can be carried out with the Hencken burner. The burner produces a lot of tiny diffusion flames at the exit of the burner. In the region around 100 mm above the burner, all these tiny diffusion flames merge together and form the adiabatic equilibrium condition. The temperature and species concentration

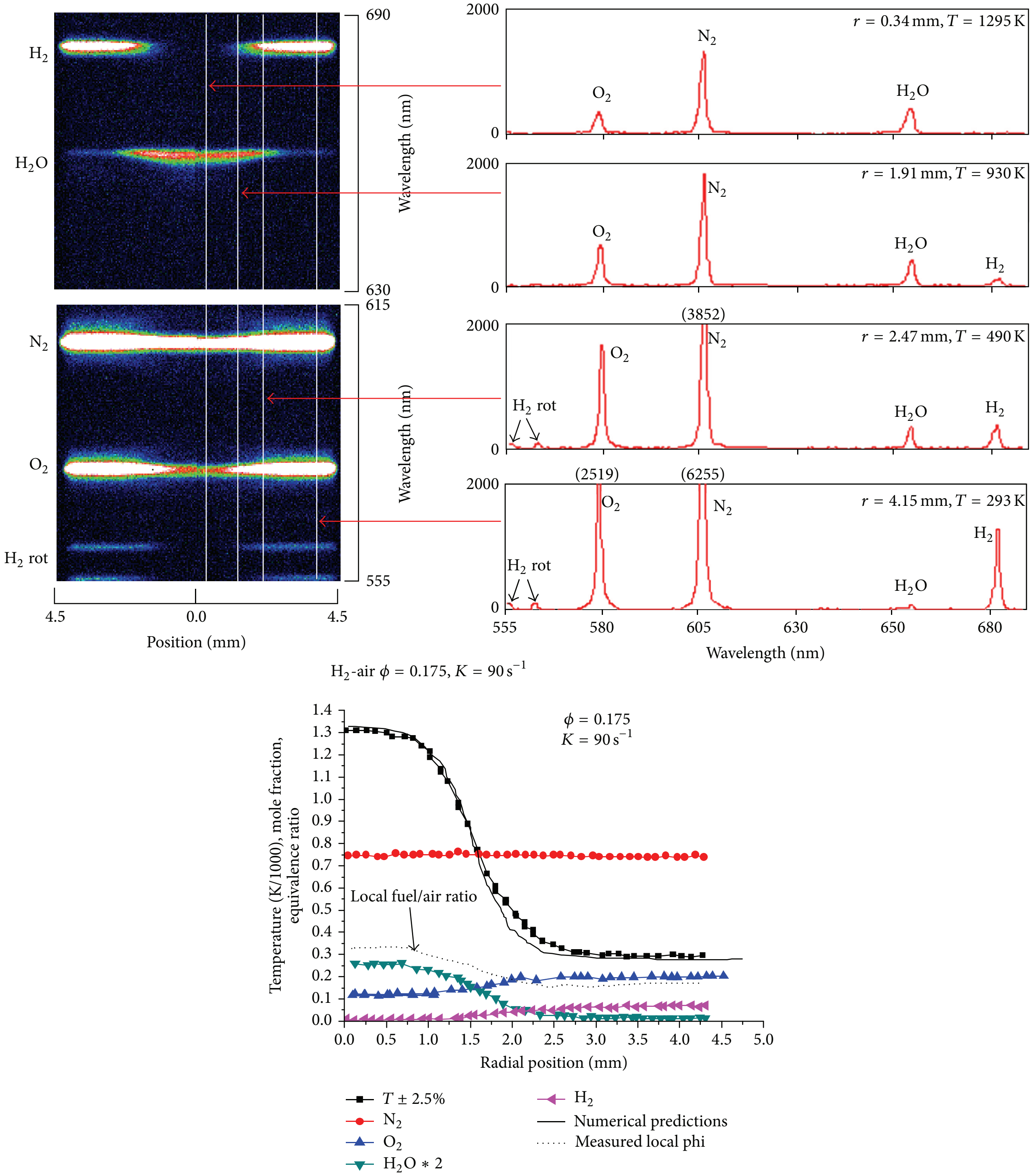

Figure 9: The experimental image, integrated spectrum, and comparison between simulation and experimental data.

in this region can be calculated with Chemkin Equil. With calculated temperature and species concentration, the Raman scattering system can be calibrated and validated.

The research team has used the visible Raman scattering system of Vanderbilt University to measure the detailed structure of H_2/air tubular flames. The collected Raman signal image and integrated signal curves are shown in Figure 9. The measured flame structure was used to validate the numerical simulation. As shown in Figure 9, the simulation is very accurate and has perfect agreement with the measured data.

The research group at Vanderbilt University also used the UV Raman system [29] to measure the species concentration

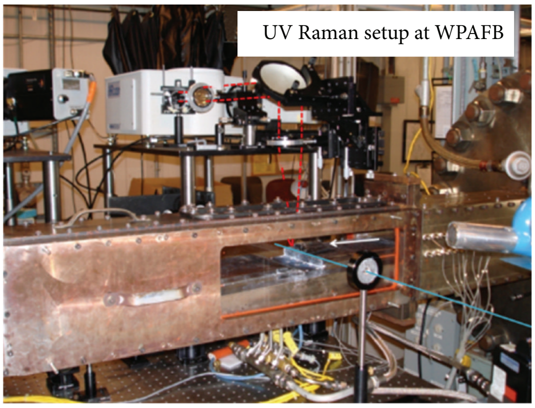

Figure 10: UV Raman setup at WPAFB [29].

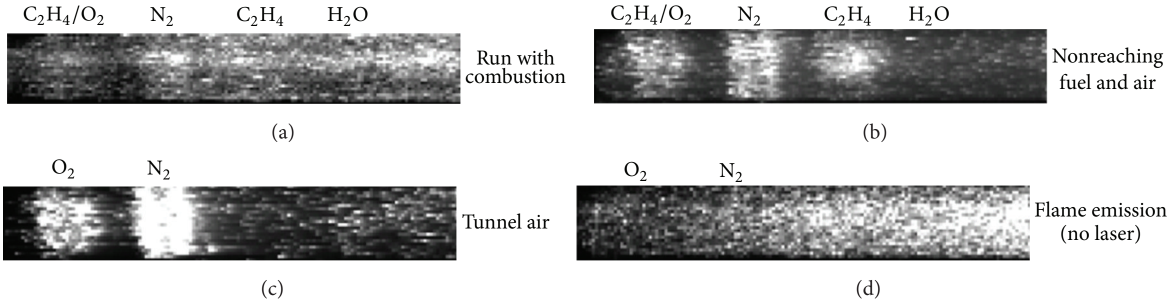

Figure 11: Images in a fuel rich region of Mach 2 flow [29].

inside a supersonic cavity combustor in Wright-Patterson Air Force Base (WPAFB) as in Figures 10 and 11. This kind of measurement in real devices is very important to understand the working mechanism of the device and calibrate and validate the CFD simulations. Particularly, in the supersonic or hypersonic reacting flow field, there is no other method to perform this kind of measurement.

6. Molecule Tagging Velocimetry (MTV)

6.1. Principle of MTV. The high speed and high temperature feature inside the combustor of aeroengine excludes the measurement methods that disturb the flow field severely. The relatively mature velocity measurement methods of laser diagnostics are particle based velocimetry including LDV (Laser Doppler Velometer), PIV (Particle Image Velocimetry), and PDV (Planar Doppler Velocimetry) [6, 30]. These methods use the solid particles much larger than molecule size; the particles are under the drag force, virtual mass force, and basset force; the result of these forces is negligible in the low speed flow field and the particle movement reflects the fluid molecule movement quite accurately.

To overcome the disadvantages of the above-mentioned particle based velocimetries, scientists have tried a lot of advanced laser diagnostic technology. Particularly, scientists have invented the Molecular Tagging Velocimetry (MTV) method for velocity measurement and applied it for supersonic combustion [30, 31].

The MTV method uses laser grid to mark specific flow molecule or atom; after a specified time delay (microseconds), another plane laser is excited to read the location of the marked molecules. The node location difference between the marking grid and the reading grid gives out two-dimensional travel distance of the excited molecules. Dividing by the specified time delay, two-dimensional velocity of the grid nodes is obtained. The tagging molecule has multiple choices such as NO, NO_2, Na, C_3H_6O, and $C_4H_6O_2$. However, these species are costly or toxic; they are not good for application. The combustion laser diagnostic group at Vanderbilt University found a perfect tagging molecule: the OH radical resulting from dissociation of water vapor. Since water vapor is everywhere, in the air and in the combustion product, there is no need for adding extra tagging molecule in the flow field. This Molecular Tagging Velocimetry is called Hydroxyl Tagging Velocimetry (HTV). A brief description of HTV mechanism is stated here; more detailed information could be found in Wehrmeyer et al. [32]. The 193 nm laser passes a beam splitter forming two laser beams; then the laser beams pass through

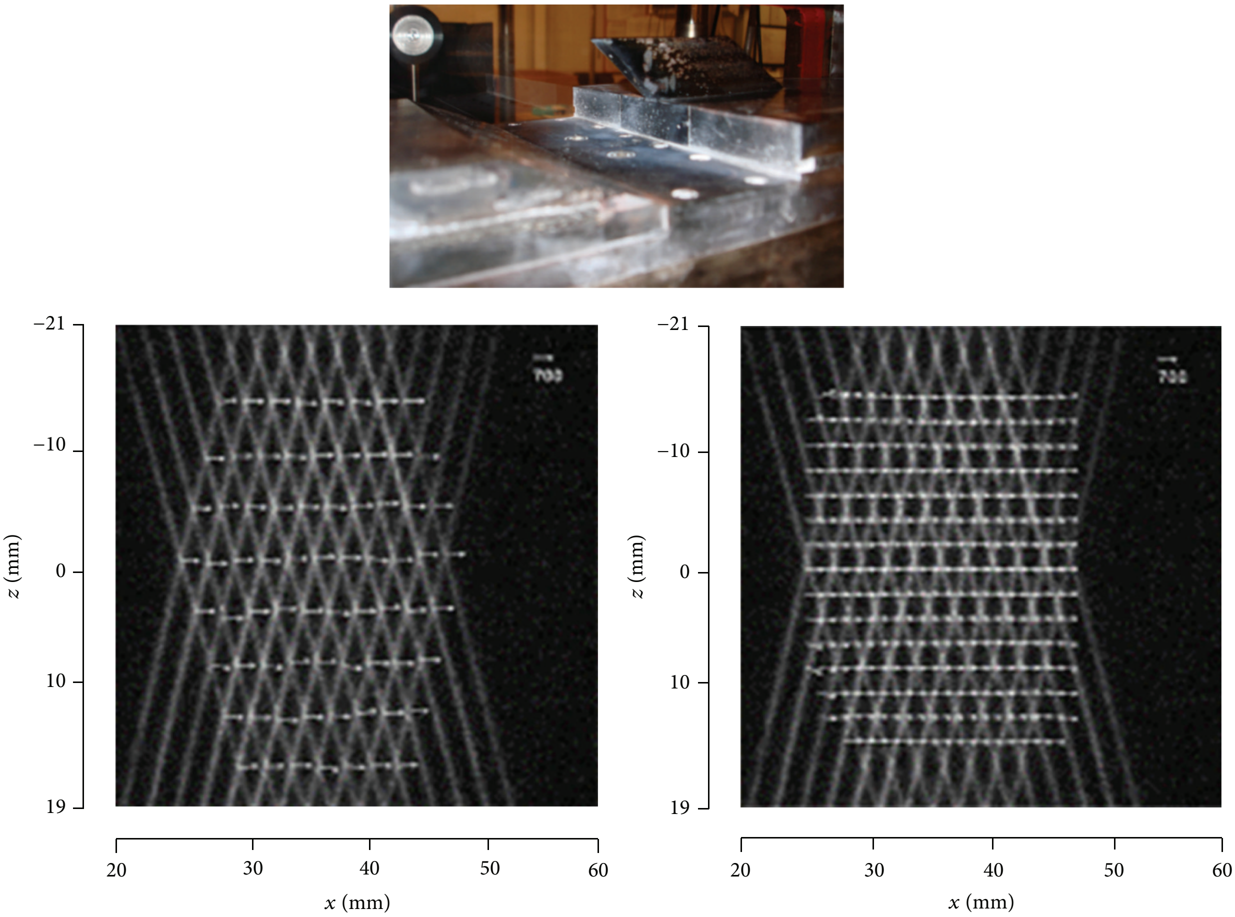

Figure 12: Picture of the supersonic cavity combustor [33].

the spherical lenses to form plane laser sheets and then pass cylindrical lenslets to form an 11 ∗ 11 laser grid. The high energy of ultraviolet laser will dissociate the H_2O to OH (tagging molecule) and H in the fluid. The original location of the tagging OH is the location of laser grid. This process is called the laser writing process. After a certain time delay, a plane laser (248 nm, 282 nm, or 308 nm) paralleling to the original grid passes the fluid in the region near the original writing location to read the new location of the generated OH through laser-induced fluorescence. This process is called laser reading process. The postprocessing software will compare the node location of the writing grid and reading grid and calculate the distance and two-dimensional velocity.

6.2. HTV Applications. There is no commercial HTV system available in the market now. It requires experienced experimentalist to design and build the system. The equipment is also very expensive. However, the benefit of this technology is so attractive that it has already been used in the aeronautical and astronautical industry since its first appearance. Professor Pitz's group at Vanderbilt University measured the flow field in the supersonic combustion cavity in Wright-Patterson Air Force Base (WPAFB) laboratory [32].

Figure 12 shows the structure of the supersonic combustion cavity and Figure 13 displays the schematic of the HTV experiment system. Figure 14 shows the measured mean and RMS velocity inside the cavity.

HTV method is also appropriate for combustion flow field. The space resolution of this technology is less than 100 micrometers; the time resolution is less than 1 microsecond. The uncertainty of the measure velocity is around ±1% for high speed flow.

7. Conclusion

Different kinds of advanced laser diagnostic techniques are introduced and their potential applications in aeroengine combustor research are analyzed. All of them require no probes, no particles, and no addition of extra species and have zero disturbances to the flow field. Spontaneous laser-induced Raman scattering technology can measure multi-species concentration simultaneously and then the temperature can be calculated. After calibration and validation,

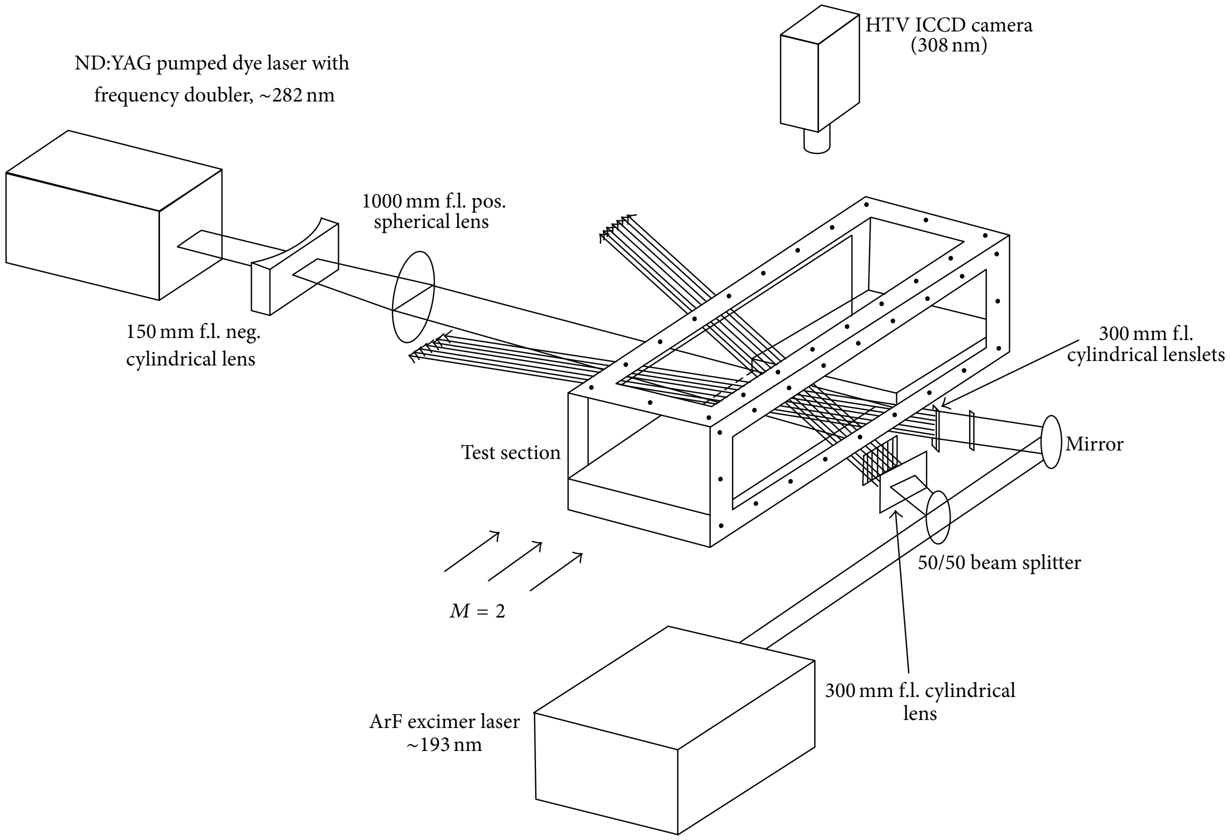

Figure 13: HTV system schematic [33].

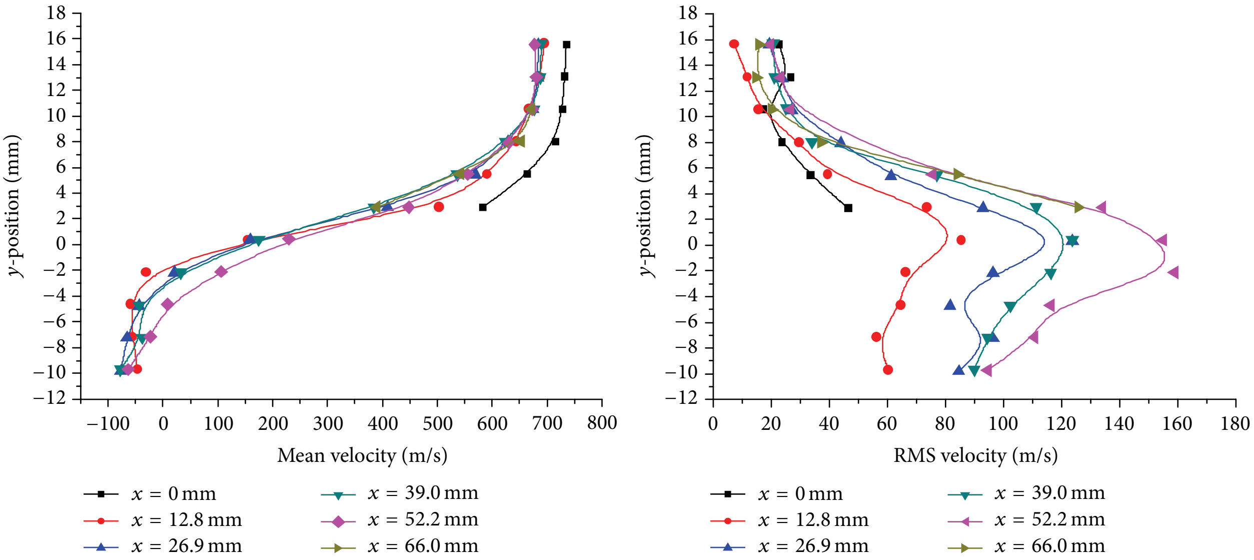

Figure 14: Measured mean and MRS velocity inside the supersonic cavity [33].

Raman scattering system has advantages over other technologies lying in broad measurement range, high time and space resolution, and tiny experimental uncertainty. The information would promote the fundamental research, design, and control of the flow field in the aeroengine combustors.

Table 1: Summary of different laser diagnostics for gas turbines.

Type	Merits	Drawbacks
PLIF	(i) It can be combined with PIV to measure the species concentration and velocity simultaneously.	(i) Fluorescence interferences are from other species, especially from hydrocarbons in high pressure reacting flows. (ii) It is difficult for quantitative measurement.
CARS	(i) CARS signal could be detected in the presence of a strong fluorescent background. (ii) Low absorption of the near-infrared excitation beams would significantly reduce the damage in samples.	(i) At very low concentrations, the advantages of the coherent addition for the CARS signal are reduced and the presence of the incoherent background becomes a problem.
RS	(i) It can measure multispecies concentration simultaneously. (ii) It has high spatial and time resolution. (iii) It has high accuracy results.	(i) The signal from a single molecule is weaker than the CARS signal. (ii) The measurement zone is only a point. (iii) The laser source is relatively expensive.
TDLAS & TDLAT	(i) Low detection limits. (ii) Determining the temperature, pressure, and velocity.	(i) Any noise introduced by the light source or the optical system will deteriorate the detectability and precision.
MTV	(i) It has high spatial and time resolution. (ii) Multipoint in the flow field is measured simultaneously. (iii) It is especially suitable for supersonic flow field measurement.	(i) The system equipment is relatively expensive. (ii) Some tagging molecule species are costly or toxic.

The summarization of the merits and drawbacks information about all the technology mentioned above are shown in Table 1.

Conflict of Interests

The authors declare that there is no conflict of interests regarding the publication of this paper.

Acknowledgments

The authors are grateful to Aeronautical Science Foundation of China (Grant no. 20132268003), National Natural Science Foundation of China (Grant no. 51406171), project supported by the Natural Science Foundation of Fujian Province (Grant no. 2015J05111), and Fundamental Research Funds for the Central Universities of China (Grant no. 2013121019) for providing the funding support for the research.

References

[1] X. Li, "Development of gas turbine and dilemma in China," *Aeroengine*, vol. 37, no. 3, pp. 1–7, 2011.

[2] E. Zhang, "On China's military aviation engine development thinking," *Aeroengine*, vol. 27, p. 1, 2001.

[3] Y. Liu, "Prospective development of Aeroengine technology," *Aeroengine*, vol. 37, p. 1, 2011.

[4] H. Wang, "Based research on aeroengine test technology," *Measurement & Control Technology*, no. 2, p. 1, 1983.

[5] Y. Chen and G. Chen, "Development of high temperature test technology on aeroengine," *Journal of Propulsion Technology*, vol. 17, p. 9, 1996.

[6] M. Mao, C. Huang, and X. Shi, "Laser temperature measurement technology of advanced aero-engine combustor test," *Measurement & Control Technology*, vol. 29, p. 92, 2010.

[7] J. M. Seitzman and R. K. Hanson, "Planar fluorescence imaging in gases," in *Instrumentation for Flows with Combustion*, p. 405, Academic Press, Cambridge, Mass, USA, 1993.

[8] B. K. McMillin, M. P. Lee, and R. K. Hanson, "Planar laser-induced fluorescence imaging of nitric oxide in shock tube flows with vibrational nonequilibrium," in *Proceedings of the AIAA 21st Fluid Dynamics, Plasma Dynamics and Lasers Conference*, Seattle, Wash, USA, June 1990.

[9] J. H. Frank, M. F. Mille, and M. G. Allen, "Imaging of laser-induced fluorescence in a high-pressure combustor," in *Proceedings of the 37th AIAA Aerospace Sciences Meeting and Exhibit*, Reno, Nev, USA, January 1999.

[10] R. K. Hanson, "Advanced laser diagnostics for reactive flows," in *Proceedings of the 40th AIAA Aerospace Sciences Meeting & Exhibit*, Reno, Nev, USA, January 2002.

[11] H. Seyfried, G. Sarner, A. Omrane et al., "Optical diagnostics for characterization of a full-size fighter-jet afterburner," in *Proceedings of the ASME Turbo Expo: Power for Land, Sea, and Air*, pp. 813–819, Reno, Nev, USA, June 2005.

[12] R. Sadanandan, M. Stöhr, and W. Meier, "Simultaneous OH-PLIF and PIV measurements in a gas turbine model combustor," *Applied Physics B*, vol. 90, no. 3-4, pp. 609–618, 2008.

[13] W. M. Tolles, J. W. Nibler, J. R. McDonald, and A. B. Harvey, "A review of the theory and application of coherent anti-Stokes Raman spectroscopy (CARS)," *Applied Spectroscopy*, vol. 31, no. 4, pp. 253–272, 1977.

[14] A. M. Zheltikov, "Coherent anti-stokes Raman scattering: from proof-of-the-principle experiments to femtosecond CARS and higher order wave-mixing generalizations," *Journal of Raman Spectroscopy*, vol. 31, no. 8-9, pp. 653–667, 2000.

[15] H. T. Beier, G. D. Noojin, and B. A. Rockwell, "Localized thermal mapping using coherent anti-Stokes Raman spectroscopy," *Journal of Biomedical Optics*, vol. 17, no. 8, Article ID 080501, 2012.

[16] A. C. Eckbreth, "CARS thermometry in practical combustors," *Combustion and Flame*, vol. 39, no. 2, pp. 133–147, 1980.

[17] L. R. Boedeker and G. M. Dobbs, "CARS temperature measurements in sooting, laminar diffusion flames," *Combustion Science and Technology*, vol. 46, no. 3–6, pp. 301–323, 1986.

[18] T. J. Anderson and A. C. Eekbreth, "Simultaneous CARS measurements of temperature and H_2, H_2O concentrations in hydrogen-fueled supersonic combustion," in *Proceedings of the 28th Aerospace Sciences Meeting*, Reno, Nev, USA, January 1990.

[19] O. Jarrett Jr., M. W. Smith, R. R. Antcliff et al., "CARS temperature measurements in a hypersonic propulsion test facility," Tech. Rep. N92-12049, NASA, 1992.

[20] A. Zumbusch, G. R. Holtom, and X. S. Xie, "Three-dimensional vibrational imaging by coherent anti-stokes Raman scattering," *Physical Review Letters*, vol. 82, no. 20, pp. 4142–4145, 1999.

[21] T. Ichimura, N. Hayazawa, M. Hashimoto, Y. Inouye, and S. Kawata, "Tip-enhanced coherent anti-stokes raman scattering for vibrational nanoimaging," *Physical Review Letters*, vol. 92, no. 22, Article ID 220801, 2004.

[22] D. T. Cassidy and J. Reid, "Atmospheric pressure monitoring of trace gases using tunable diode lasers," *Applied Optics*, vol. 21, no. 7, pp. 1185–1190, 1982.

[23] P. Zorabedian, "Tunable external-cavity semiconductor lasers," in *Tunable Lasers Handbook*, p. 349, Academic Press, Cambridge, Mass, USA, 1996.

[24] P. Werle, F. Slemr, K. Maurer, R. Kormann, R. Mücke, and B. Jänker, "Near- and mid-infrared laser-optical sensors for gas analysis," *Optics and Lasers in Engineering*, vol. 37, no. 2-3, pp. 101–114, 2002.

[25] K. M. Busa, E. N. Ellison, B. J. McGovern et al., "Measurements on NASA langley durable combustor rig by TDLAT: preliminary results," in *Proceedings of the 51st AIAA Aerospace Sciences Meeting Including the New Horizons Forum and Aerospace Exposition*, AIAA 2013-0696, Grapevine, Tex, USA, January 2013.

[26] K. M. Busa, E. Bryner, B. J. McGovern et al., "Demonstration of capability of water flux measurement in a scramjet combustor using tunable diode laser absorption tomography and stereoscopic PIV," in *Proceedings of the 49th AIAA Aerospace Sciences Meeting Including the New Horizons Forum and Aerospace Exposition*, AIAA 2011-1294, Orlando, Fla, USA, January 2011.

[27] K. M. Busa, J. C. McDaniel, M. S. Brown, and G. S. Diskin, "Implementation of maximum-likelihood expectation-maximization algorithm for tomographic reconstruction of TDLAT measurements," in *Proceedings of the 52nd Aerospace Sciences Meeting*, AIAA 2014-0985, National Harbor, Md, USA, January 2014.

[28] P. Wang, "Investigation of stretch and curvature effects on flames," in *Experimental and Numerical Study of Tubular Premixed Hydrocarbon Flames*, Vanderbilt University, Nashville, Tenn, USA, 2006.

[29] R. W. Pitz, N. R. Grady, S. W. Shopoff et al., "UV Raman scattering measurements of a mach 2 reacting flow over a piloted cavity," in *Proceedings of the 46th AIAA Aerospace Sciences Meeting and Exhibit*, AIAA-2008-0244, Reno, Nev, USA, January 2008.

[30] W. Hu, B. Zhang, D. Wang, and Y. Dou, "The development of laser diagnostics in the aeroengine measurement field," *Measurement & Control Technology*, vol. 36, no. 2, pp. 50–54, 2010.

[31] K. Kohse-Höinghaus, R. S. Barlow, M. Aldén et al., "Combustion at the focus: laser diagnostics and control," *Proceedings of the Combustion Institute*, vol. 30, no. 1, pp. 89–123, 2005.

[32] J. A. Wehrmeyer, L. A. Ribarov, D. A. Oguss, and R. W. Pitz, "High temperature flow tagging velocimetry with 193 nm H_2O photodissociation," *Applied Optics*, vol. 38, no. 33, pp. 6912–6917, 1999.

[33] R. W. Pitz, M. D. Lahr, Z. W. Douglas et al., "Hydroxyl tagging velocimetry in a supersonic flow over a cavity," *Applied Optics*, vol. 44, no. 31, pp. 6692–6700, 2005.